Evaluation of Energy Parameters and Pollutant Gases for Apple Drying in Refractance Window Solar Dryer Equipped with a PTC Solar Collector

M. Teymori-Omran[1], E. Askari Asli-Ardeh[1*], A. Motevali[2], E. Taghinezhad[3]

1- Department of Biosystem Engineering, University of Mohaghegh Ardabili, Ardabil, Iran
2- Department of Biosystem Engineering, Sari Agricultural Sciences and Natural Resources University, Sari, Iran
3- Department of Biosystem Engineering, Faculty of Agriculture, Tarbiat Modares University, Tehran, Iran
(*- Corresponding Author Email: ezzataskari@uma.ac.ir)
https://doi.org/10.22067/jam.2024.90300.1298

Abstract

In this study, the drying process of apples was explored using a new combined solar dryer known as the Refractance Window-Parabolic Trough Collector (RW-PTC). The drying kinetics, energy efficiency in the solar collector and dryer, and the role of the dryer in reducing energy consumption and pollutant emissions during the drying process were investigated. Drying experiments were carried out with three energy sources, including conventional non-renewable energy (RW), solar-assisted drying (PRW), and fully solar drying (SRW). In the first and second methods (RW and PRW), drying was performed at three temperature levels (65, 75, and 85 °C), and in the third method (SRW), drying was performed at the temperature of the solar collector. The average optical and thermal efficiency of the PTC collector during the experimental hours were 62.01% and 49.31%, respectively. The lowest specific energy consumption was observed in the SRW method at 10.24 (kWh kg^{-1}). The results showed that the solar energy used in the combined drying methods of PRW-65, PRW-75, PRW-85, and SRW accounted for 54.91%, 52.62%, 48.85%, and 70.30% of the total energy consumption, respectively, and by the same amount, energy consumption from non-renewable sources was reduced. By using a solar collector in the PRW and SRW drying methods, the CO_2 emission was reduced by 54.64% and 80.94%, respectively, compared to the conventional RW method. Overall, the implementation of solar energy in the PRW and SRW methods improved energy parameters and reduced pollutant emissions during the drying process.

Keywords: Apple drying, parabolic trough collector, Refractance window, Solar dryer

Introduction

The solar-assisted drying of agricultural products has been practiced since ancient times by spreading the produce under direct sunlight. However, this method faced challenges such as insect and bird infestation, sudden weather changes, prolonged drying times, sunburn, lack of control over drying conditions, and deterioration in product quality (Tiwari, Tiwari, & Al-Helal, 2016). Over time, solar dryers were developed to improve the final product quality in a controlled environment. Cabinet dryers, solar-assisted hybrid dryers, and greenhouse dryers are among the recognized solar dryers (Kumar & Singh, 2020). Research has shown that most solar dryers are based on convective dryers and work by exposing the product to a hot air stream (direct and indirect). Only a limited number of solar dryers employ alternative methods. Among the older dryers, convection dryers were most widely used due to their simple construction and low cost. Poor energy efficiency, low quality of the final product, and prolonged drying time are major drawbacks of industrial convection dryers. These dryers also operate using fossil fuels, which contribute to environmental issues (Onwude, Hashim, Abdan, Janius, & Chen, 2019; Teymori- Omran *et al.*, 2023). With technological advances in dryer production, new generations[1] of dryers have emerged. Refractance Window dryer is one of the fourth-generation dryers, which is similar to freeze dryer in terms of final product quality. Refractance window dryers utilize near-boiling

1- The first generation of dryers includes cabinet, tray, conveyor, and tunnel dryers. The second-generation includes technologies such as spray, fluidize bed, and drum dryers. The third generation includes freeze and osmosis dryers, while the fourth generation comprises microwave, refractance window, and radio frequency dryers.

hot water to dry thin layers of products, unlike convective dryers that use hot air (Mahanti *et al.*, 2021; Raghavi, Moses, Anandharamakrishnan, 2018). In recent years, considerable attention has been paid to these dryers, and research has been conducted in this topic. For example, in a study, apples were dried using a combined refractance window-infrared dryer. The results showed that the drying time was reduced by 50% compared to the conventional refractance window method and by 69% compared to the hot air-drying method (Rajoriya, Shewale, Bhavya, & Hebbar, 2020). A study investigates the mass transfer parameters and quality of dried apples using the refractance window method. The results indicated that the drying time was shorter, and the residual amount of ascorbic acid was higher when compared to hot air drying (Rajoriya, Shewale, & Hebbar, 2019). Additionally, the satisfactory performance of RW dryers in drying agricultural products has been reported in other studies (Caparino et al., 2012; Padhi & Dwivedi, 2022; Waghmare, 2021). A review indicates that RW dryers have favorable quality conditions, but some problems exist, such as their high energy consumption. Although limited research has been done on energy consumption in RW dryers, it is clear that heating water to near boiling temperatures, due to its high heat capacity, consumes a significant amount of energy. Currently, this energy is supplied by fossil fuels and electric or gas heaters. A suitable solar collector is necessary to utilize solar energy in these systems. Flat plate solar collectors or photovoltaic-thermal collectors have been used in research for dryers, but due to their operating temperature (usually between 50 to 70 °C), large-scale development for drying is not feasible (Seyfi, Asl, & Motevali 2021; Teymori-omran, Motevali, Seyedi, & Montazeri, 2021). Parabolic Trough Collectors (PTC) are among the best collectors for receiving solar energy and are widely used with high capacity in industries and solar power plants. Extensive research has been conducted on PTC collectors in recent years (Gharehdaghi, Moujaes, & Nejad, 2021; Manikandan, Iniyan, & Goic, 2019; Wang, Yao, Shen & Yang, 2023). In several research studies conducted in recent years, these systems have been used in combination to provide energy for first and second-generation dryers (Camci, 2020; Sookramoon, 2016). All these studies demonstrate the high quality of PTC systems in receiving and storing solar energy and its application to the drying process. On the other hand, considering the energy supply issues in RW dryers (heating water to high temperatures for drying), the use of PTC collectors as a clean solar energy source in this study has been considered. This study presents an innovative approach by utilizing a PTC solar collector to supply energy for the drying process in a refractance window (RW) dryer, creating a combined RW-PTC system. The goal is to supply the necessary energy for the RW dryer while drying apple slices, using a well-designed small-scale PTC collector. This research investigates the potential integration of clean solar energy into the refractance window drying method for minimizing the emission of polluting gases.

Materials and Methods

In this study, a combined solar system of the RW-PTC type was utilized. The system consisted of two components: a parabolic trough collector (PTC) and a Refractance Window (RW) dryer (Figure 1). The RW dryer is designed to utilize both utility electricity and the heat collected by the PTC collector to warm the water. Water is pumped from the main reservoir into the solar collector, where it is heated, and then returned to the reservoir. Water from the main reservoir flows into a smaller tank that contains an electric heater, before entering the hot water tank in the RW compartment. An RW dryer and a PTC system were used on a laboratory scale for this research, as depicted in Figure 1. In the PTC system, the reflective part consisted of 40 mirrors (50×1000 mm) with a receiver made of vacuum tubes coated with a solar absorber and covered in glass. The PTC collector was positioned east-west at a geographic location

with a longitude of 53° 5' and latitude of 36° 4', at an altitude of 54 m (in Sari city, northern Iran, Mazandaran province). To prevent excessive heat buildup, a low concentration ratio (CR = 6)[1] was chosen for the solar system. For drying, an RW dryer on a small scale (200×300 mm) was employed a small centrifugal fan was installed on top of it to extract moisture from the compartment. The bath walls were made of stainless steel to prevent heat loss, and the lower section, sides of the basin, as well as the inlet and outlet pipes of the RW and PTC systems, were insulated to prevent heat loss.

A layer of Mylar plastic (PET[2], 0.2 mm thickness) was placed on top of the basin, and its surroundings were completely waterproofed. Apple slices were uniformly placed on the plastic surface to cover the entire surface. This drying setup was placed inside a larger enclosure. Table 1 provides further details of the RW-PTC system employed. The experiments were conducted from 10:00 AM to 3:00 PM, and the device was turned on half an hour before starting to reach stable conditions. The data recording interval was set to 10 minutes.

Sample preparation

In this research, uniform-sized and similarly ripened Ginger Gold variety apples were carefully selected for the study. After procuring the apples from local markets (in Mazandaran province, northern Iran), they were stored in a refrigerator at 4 °C until the start of the experiments. To measure the initial moisture content, 150 grams of fresh apple samples were placed in the oven at a temperature of 103 °C (Mahanti *et al.*, 2021). In the drying experiments, samples were prepared from horizontal slices of the apples using a household slicer with a thickness of 3 mm, and each sample weighed 70 g. The drying experiments reduced the moisture content from 85% to below 20% on a wet basis and were divided into three categories: conventional Refractance window drying (RW), solar combined drying (PRW), and fully solar drying (SRW). In the first category, conventional refractance window (RW) drying experiments were conducted. For these experiments, grid electricity was used to heat the water, and solar energy was not utilized. The experiments were conducted at three temperature levels (65, 75, and 85 °C). In the second category, combined drying experiments with solar energy assistance (PRW) were conducted. Similarly, three temperature levels (65, 75, and 85 °C) were used. In this method, the water temperature in the system reached 60°C using a solar collector, and then an electric heater (grid electricity) was used to reach the desired temperature levels [3] (65, 75, and 85 °C), after which the electric heater was turned off, and heat was supplied until the end of the drying process by the solar collector. In the third category of experiments (SRW), all the energy required for heating the water was supplied solely by the solar collector, and the drying temperature varied throughout the process depending on the temperature of the solar collector. In this method, the samples were placed inside the dryer after reaching a temperature of 60 °C. After the product was added to the dryer, the system temperature increased to about 70 °C. During most of the drying process, the inlet temperature to the dryer was in the range of 65-70 °C. The water flow rate was 3 L min^{-1} for all drying experiments in the dryer and 15 L min^{-1} in the solar system. The experiments continued until the moisture content of the product reached below 20% (w. b.). The dimensionless moisture ratio (MR) is a crucial concept in the study of drying processes. Equation 1 specifies the dimensionless moisture ratio (Onwude *et*

1- The concentration ratio is the ratio of the apparent surface area of the concentrator to the external surface area of the receiver (CR =Aac/Aro). This ratio is around 15 and above (Awan *et al.*, 2020). The selection of 6 is based on its ability to facilitate easier control of water temperature, eliminating the need for cooling systems.

2- Polyethylene terephthalate

3- The water temperature in refractance window drying studies is usually chosen close to the boiling point; for example, 60, 70, 80, or 90 °C (Shahraki, Khojastehpour, Golzarian, & Azarpazhooh, 2024)

al., 2019). Where M represents the moisture content at drying time, M_0 represents the initial moisture content, and M_e is the equilibrium moisture content.

$$MR = \frac{M-M_e}{M_0-M_e} \quad (1)$$

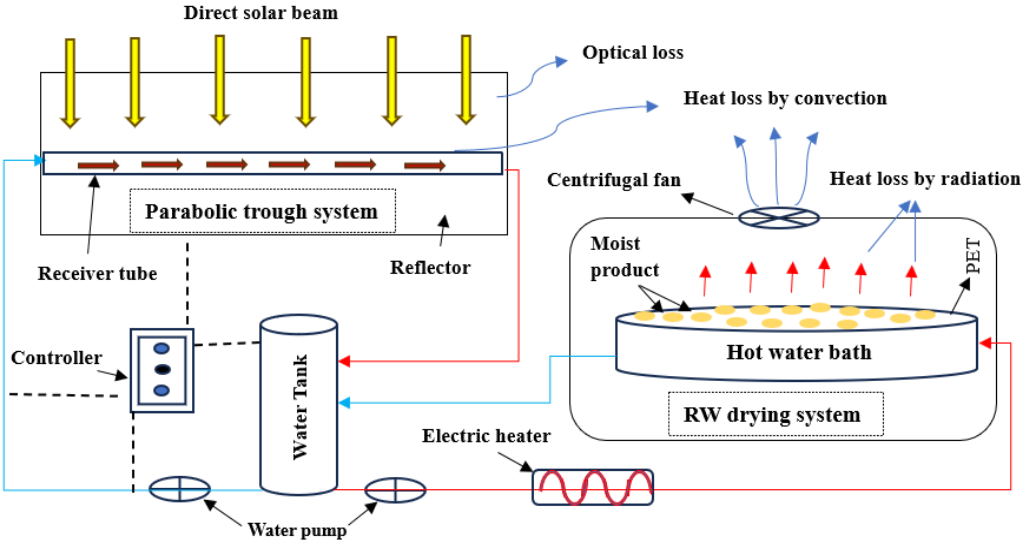

Fig. 1. The RW-PTC combined dryer system utilized in this research, along with its real and the schematic images

Table 1- Dimensions and coefficients related to RW-PTC solar dryer

Part	Parameter	Value	Unit
Concentrator	Concentrator dimensions (length × width)	2000×1000	mm
	Focal length (f)	280	mm
	Parabola width (W)	750	mm
	Rim angle (ϕ_r)	70	°
Receiver	Outer diameter (D_{ro})	58	mm

	Inner diameter (D_{ri})	40	mm
	Total reflection coefficient (ρ_T)	0.8	-
	Cover glass transmission coefficient (τ)	0.95	-
	Absorption coefficient (ω)	0.95	-
	Interception coefficient (γ)	1	-
Working fluid	Flow rate (m)	0.3	kg s^{-1}
	Specific heat capacity (C)	4200	J kg^{-1} °C^{-1}
Dryer	Dimensions of the dryer chamber	400×600×300	mm
	The dimensions of the hot water container	40×200×300	mm

Thermal and Optical Efficiency of PTC

PTC solar collectors utilize only direct solar radiation. Therefore, the total available radiation on the collector is obtained from Equation (2). Errors in receiving radiation on the concentrator and its receiver led to incomplete capture of reflected radiation, which is due to construction flaws in the concentrator and issues with sunlight tracking. Consequently, the absorbed heat (Q_S) depends on the available radiation and the optical efficiency of the collector (η_{opt}), as obtained from Equation (3). In this equation, Q_S and G_b are the total available radiation and the intensity of direct solar radiation, respectively (Awan, Khan, Zubair & Bellos, 2020; Bellos & Tzivanidis, 2018).

$$Q_S = A_{ac}.G_b \quad (2)$$

$$Q_{abs} = Q_S \,.\eta_{opt} \quad (3)$$

The optical efficiency of the collector largely depends on the angle of incidence of solar rays and is obtained from Equation (4).

$$\eta_{opt} = X(\theta) \,.\eta_{opt-max} \quad (4)$$

where, $X(\theta)$ is the angle correction factor. The cosine of the angle (θ) for PTC placed in an east-west direction is obtained from Equation (6) (Gaul & Rabl, 1980). In this equation, α is solar declination angle and β is solar hour angle.

$$X(\theta) = \cos(\theta) - \frac{f}{l} \,.\left(1 + \frac{W^2}{48\, f^2}\right) .\sin(\theta) \quad (5)$$

$$\cos(\theta) = (1 - \cos^2(\alpha) \,.\sin^2(\beta))^{1/2} \quad (6)$$

The declination angle for any day of year (N) can be calculated approximately by Equation (7), and hour angle can be calculated by Equation (8), where the plus sign applies to afternoon and minus sign to morning hours (Kalogirou, 2023):

$$\alpha = 23.45 \,\sin\left[\frac{360}{365}(284 + N)\right] \quad (7)$$

$$\beta = \pm 0.25\ (Number\ of\ minutes\ from\ local\ solar\ noon) \quad (8)$$

$$\eta_{opt-max} = \rho_T \,.\gamma \,.\tau \,.\omega \quad (9)$$

Equation (9) is used to determine the maximum optical efficiency value. In this equation, ρ_T is the overall reflectance coefficient, including tracking errors, transmittance coefficients, and other factors that cause optical losses. Additionally, τ is the transmittance coefficient of the cover glass, ω is the absorber absorption coefficient, and γ is the tracking loss coefficient (Bellos & Tzivanidis, 2020; Gaul & Rabl, 1980). According to Equation (10), the absorbed energy by the receiver is converted into two parts: useful heat (Q_u) and heat loss (Q_{loss}). Only a portion of the solar energy is received by the fluid, referred to as useful heat or received energy of the collector, as obtained from Equation (11). Finally, the thermal efficiency of the PTC collector (η_{th}), one of the most important performance indicators of a solar collector, is obtained from Equation (12) (Awan *et al.*, 2020; Bellos & Tzivanidis, 2020; Gaul & Rabl, 1980).

$$Q_{abs} = Q_u + Q_{loss} \quad (10)$$

$$Q_u = \dot{m} \,.C_{P,w}(T_{out} - T_{in}) \quad (11)$$

$$\eta_{th} = \frac{Q_u}{Q_S} \quad (12)$$

Table 2- Specifications of the devices used in this research

Instrument	Specification
Water pump	3 L min^{-1}, 20 W, 12 V DC, 18 L min^{-1}, 60 W, 220 V AC
Flow rate sensor	Model: YFS-201, Range 0.5-20 L
Data logger Thermometer	Model: TES, PROVA800
Temperature sensor	Range 0-900 °C, Accuracy ± 1 °C
Digital balance	Range 0-600 g, Accuracy ± 0.01 g
Centrifugal fan	12×12, 12 V DC
DC motor (Tracking system)	24 V DC, 10 A
Power supply (Tracking system)	360 W, 24 V, 15 A
Light Dependent Resistor	3 photocells, single-axis tracking (north-south)
Pyranometer (Solar Power Meter)	Model: SPM-1116SD, Accuracy 0.1 W m^{-2}
Wattmeter	Range 0-9999 W, Accuracy ± 1 W

Energy Efficiency in RW Dryer

The heat received by a dryer is either used to increase the product temperature and evaporate moisture from the product or is lost to the environment. Therefore, the heat balance in an RW dryer is represented by Equation (13). In this equation, T_{do} and T_{di} are the temperatures of water at the inlet and outlet of the dryer, respectively. On the right side of the equation, Q_P is the heat required to increase the product temperature, Q_e is the heat required for moisture evaporation, and $Q_{l,d}$ is the heat loss from the product surface (Baeghbali, Niakousari, & Farahnaky, 2016; Raghavi *et al.*, 2018).

$$Q_d = \dot{m} \,.\, C_{P,w} \,.\, (T_{do} - T_{di}) = Q_P + Q_{ev} + Q_{l,d} \quad (13)$$

The heat quantity used for increasing the product temperature (Q_P) and the heat quantity used for moisture evaporation (Q_{ev}) are obtained from Equations (14) and (15), respectively. In these equations, m_p is the mass of the product (apple slices), $C_{P,p}$ is the specific heat capacity of the product (assumed 3.6 kJ kg^{-1} C^{-1}), ΔT is the temperature increase of the product, and λ_l is the latent heat of evaporation (assumed 2400 kJ kg^{-1}) (Baeghbali et al, 2016; Raghavi *et al.*, 2018).

$$Q_P = m_p \,.\, C_{P,p} \,.\, \Delta T \quad (14)$$

$$Q_{ev} = \lambda_l \,.\, Drying\ rate \quad (15)$$

The energy efficiency of the system is defined as the energy consumed to remove moisture from the product divided by the net input energy, according to Equation (16). Specific energy consumption is defined as the amount of energy consumed per kilogram of moisture evaporated from the product (Equation 17), and the specific moisture extraction rate (SMER) represents the ratio of the mass of evaporated water to the total energy consumed by the dryer, obtained from Equation (18) (Beigi, 2016; Mohammadi, Tabatabaekoloor, & Motevali, 2019; Motevali, Minaei, Banakar, Ghobadian, & Khoshtaghaza, 2014).

$$\eta_e = \frac{Q_{ev}}{net\ energy\ input(renewable + nonrenewable)} \quad (16)$$

$$SEC = \frac{net\ energy\ input(renewable + nonrenewable)}{(m_i - m_f)} \quad (17)$$

$$SMER = \frac{(m_i - m_f)}{net\ energy\ input(renewable + nonrenewable)} \quad (18)$$

Finally, the drying efficiency (thermal efficiency of the dryer) is calculated as the sum of energy used for heating and evaporating moisture from the product divided by the net input energy to the system, according to Equation (19) (Nindo, Feng, Shen, Tang, & Kang, 2003; *Raghavi et al.*, 2018).

$$DE = \frac{Q_{ev} + Q_P}{net\ energy\ input(renewable + nonrenewable)} \quad (19)$$

Environmental Impacts

To evaluate the environmental impacts of

drying processes using different methods, the first step was to measure the amount of electrical energy consumption in each method. The next step is to assess the performance of power plants in supplying the energy required for the drying process. Various power plants exist in Iran to provide electricity for various sectors including industry and agriculture, with most of them being steam, gas, and combined cycle power plants. The primary fuel consumed in Iranian power plants is natural gas, with liquid fuels also being used alongside. The type of fuel used significantly affects the amount and type of pollution generated. In this study, considering the transmission coefficient of electricity from the power plant to the place of consumption (13.3%), internal consumption coefficient (3.2%), and average coefficients for pollutant generation (per kilowatt-hour of electricity produced in Iranian power plants), the number of pollutants generated in each drying process method was evaluated. The pollutants analyzed in this study include carbon dioxide, methane, sulfur dioxide, and NOx. Table 3 presents the average coefficients for pollutant generation per kilowatt-hour of electricity produced in various power plants in Iran (Nazari *et al.*, 2010; Taghinezhad, Kaveh, Szumny, Figiel, & Blasco, 2023).

Table 3- Average coefficients for the emission of polluting gases in different power plants per kWh of electricity production

Polluting gas	**NO_x**	**SO_2**	**CH_4**	**CO_2**
Coefficient (kg kW h^{-1})	2.31×10^{-3}	2.57×10^{-3}	14.97×10^{-6}	62×10^{-2}

Results and Discussions

In this study, the drying of apple slices in a combined solar dryer type of RW-PTC was investigated. Drying methods included conventional Refractance Window drying (RW), a combined drying method using solar energy (PRW), and a fully solar drying method (SRW). The image of the dried product using the RW-PTC system is shown in Figure 1. The examination of results indicated that an increase in temperature from 65 to 85 °C led to a reduction in the drying time in both conventional and combined methods. Increasing the temperature from 65 to 85 °C reduced the drying time in the RW method from 320 minutes to 140 minutes (a decrease of 56.25%), and in the combined method (PRW) from 260 minutes to 160 minutes (a decrease of 38.46%). The drying time for samples using the SRW method, which depended solely on solar energy, was 240 minutes (four hours) to reduce moisture content from 85% to below 20% on wet basis. Figure 2a illustrates the relationship between the dimensionless moisture ratio (MR) and time. In methods where the water temperature was higher than the others, such as RW-85 and PRW-85, the moisture removal rate was higher than the other methods. Similarly, in methods where the water temperature was lower, the moisture removal rate from start to finish was lower than the other methods, such as RW-65 and PRW65. This graph is slightly different from those plotted for dimensionless moisture ratio in our previous studies or studies conducted on hot air drying (Teymori-Omran *et al.*, 2023). The observed difference was in the initiation of the drying process. In hot air drying, it was observed that the moisture removal rate was initially high, then decreased, and continued to decrease as the process entered the falling rate phase of drying. However, here, the moisture removal rate started low, increased in the middle, and then declined at the end of the drying process. The slow moisture removal at the beginning of the process may be due to the delayed increase in temperature at the product surface where the water is located. It seems that due to the delay in heat transfer to the upper surface of the product, surface moisture in this area dries more slowly, which causes the moisture removal rate at the beginning of the drying process using the refractance window method to be lower than that using the hot air (convective) drying method. Figure 2b shows the changes in the inlet temperature to the

dryer. In RW methods, the water inlet temperature was maintained within the same range of 65 °C, 75 °C, and 85 °C, according to the temperature control system, with a variation of less than 2 °C. In the combined method PRW-65, the water inlet temperature rose to 71.1 °C during the day after the electric heater was turned off, due to the increase in temperature from the solar system. However, in the methods PRW-75 and PRW-85, after the electric heater was turned off, the water temperature at the dryer inlet decreased to 72.9 °C and 74.3 °C, respectively, a few hours into the drying process. Figure 2c shows the variations of radiation intensity and ambient temperature durinthe test hours. Solar radiation varied from 611-849 (W m^{-2}) during the tests.

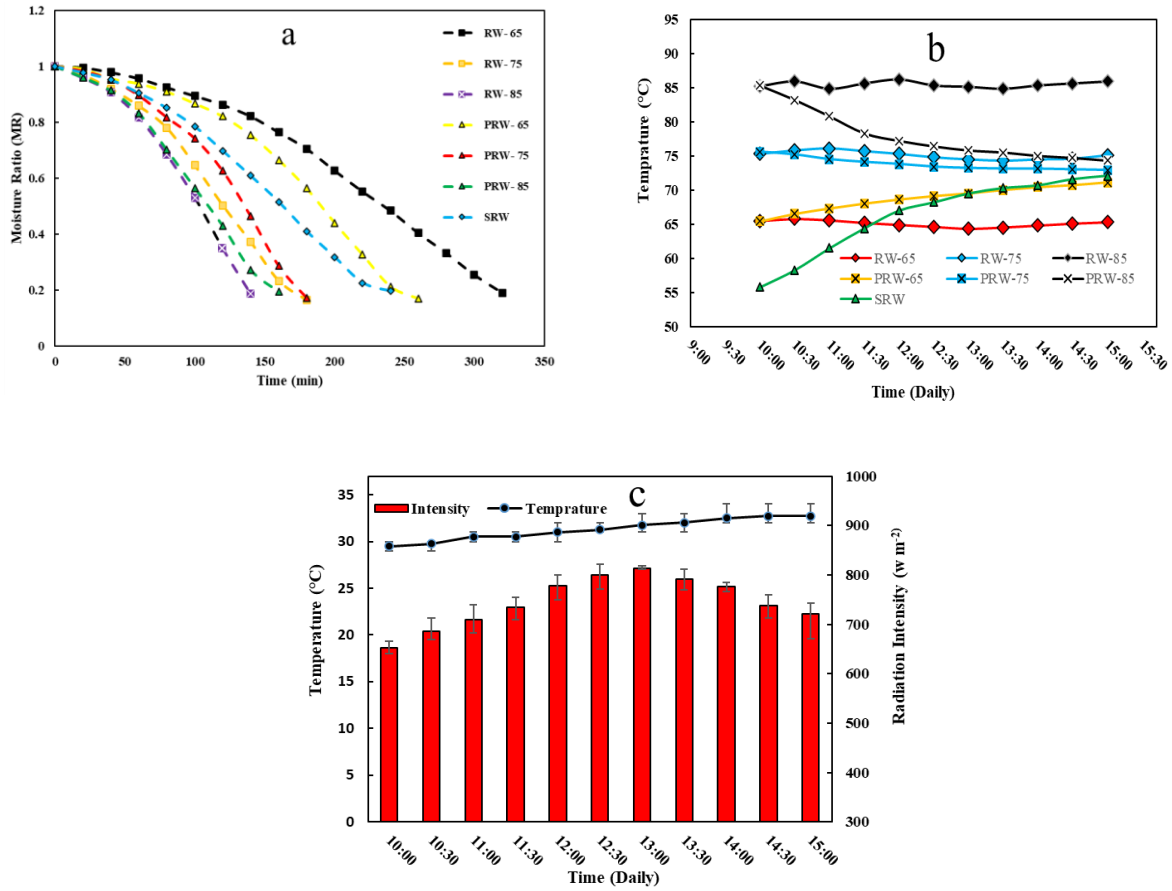

Fig. 2. (a) Dimensionless moisture ratio in the drying process, (b) The inlet temperature to the dryer in different tests, and (c) The average intensity of radiation and ambient temperature

Energy Efficiency in Solar Collectors

Optical efficiency is one of the most important parameters in the operation of a solar collector. In this study, the optical efficiency of the collector was determined based on the coefficients provided in Table 1, the geographic location of the collector, and the time of experimentation. Figure 3a illustrates the optical efficiency of the solar collector throughout the day. The average optical efficiency during the experimental hours was approximately 62.01%. The highest optical efficiency occurred at noon at 72.2%, while the lowest optical efficiency (at 15:00) was 43.8%. Generally, the optical efficiency of this collector was slightly lower than standard collectors due to the materials used, but the geographic location and experimental timing were favorable. In other studies, the optical efficiency of a commercial PTC system was found to be approximately 75% (Bellos & Tzivanidis, 2018). Thermal efficiency is one of

the most important parameters for demonstrating the performance of a PTC solar collector. The thermal efficiency of a solar collector depends on various factors such as solar radiation intensity, optical efficiency, concentration ratio ambient temperature, collector temperature, fluid temperature, and others (Shirole, Wagh, & Kulkarni, 2021). In this study, the minimum thermal efficiency of 39.68% was obtained at 10:00 a.m. and the maximum thermal efficiency of 62.96% was obtained at 13:30. The average thermal efficiency of the collector during the experimental hours was 49.31%. Figure 3b shows the thermal efficiency of the solar collector throughout the day. In the early hours of the experiment (10:00), solar radiation intensity was low, and in addition to the lower optical efficiency, the thermal efficiency was also lower than usual. As the experiment approached noon, the thermal efficiency increased, peaking between 12:30 and 13:30. The increase in thermal efficiency can be attributed to the increased solar radiation intensity and optical efficiency. Additionally, at this time, due to the increase in ambient temperature, the amount of heat loss relative to the received energy decreased, ultimately leading to an increase in thermal efficiency. Similarly, in another study, the average thermal efficiency of a PTC system was found to be 42.1% (Kajavali, Sivaraman, & Kulasekharan, 2014). In another study, the thermal efficiency of a PTC system was theoretically determined by simulating the system in the summer and winter seasons. According to the results, the thermal efficiency of the PTC system in summer and winter was 73% and 67%, respectively (Elmohlawy, Kazanjan, & Ochkov, 2018). In another study, the thermal efficiency ranged from 19.7% to 52.6% for a PTC collector (Chafie, Aissa, & Guizani, 2018).

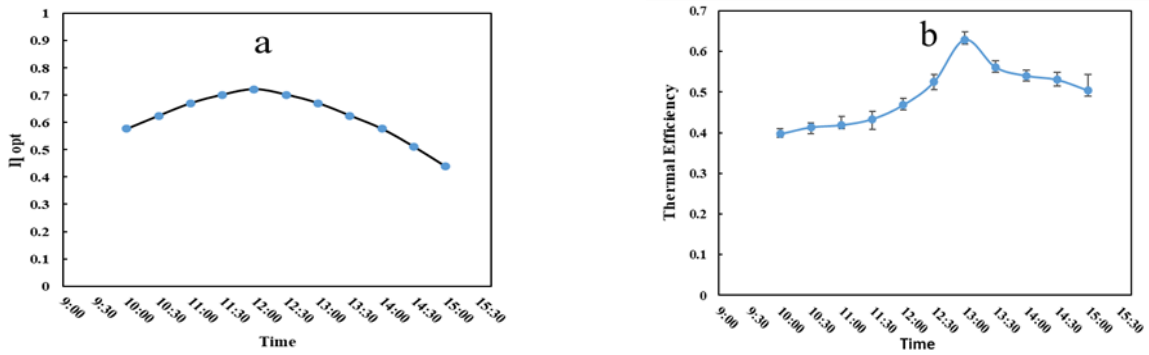

Fig. 3. (a) Average optical efficiency of PTC collector, and (b) The average thermal efficiency of the PTC collector

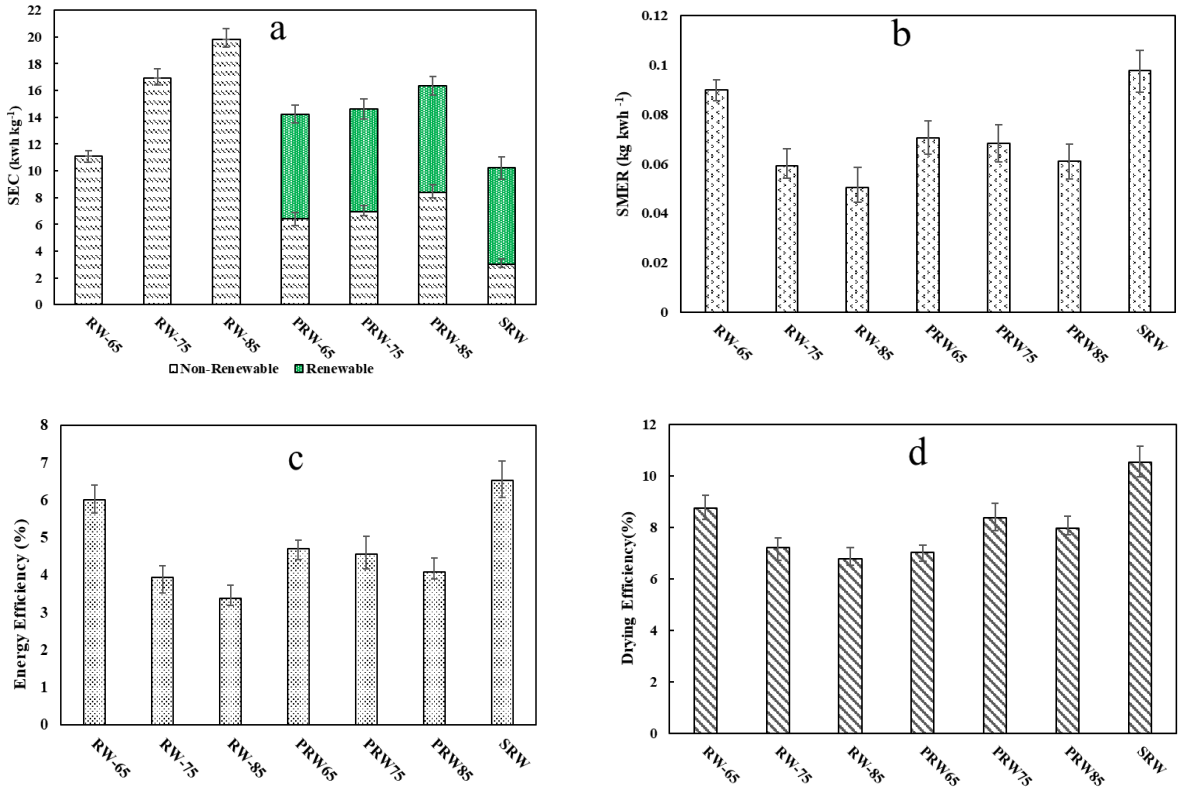

Fig. 4. (a) Specific energy consumption, (b) Specific moisture extraction rate, (c) Energy efficiency, and (d) Dryer efficiency in different drying methods

Energy Efficiency in RW Dryers

Figure 4a shows the specific energy consumption across various drying methods. In this study, the energy for drying was sourced from two supplies: solar energy and municipal electricity, which were divided into renewable and non-renewable components. In the figure, the RW-85 method showed the highest specific energy consumption at 19.82 (kWh kg^{-1}), whereas the SRW method exhibited the lowest at 10.24 (kWh kg^{-1}). The contribution of solar energy was also considered in calculating the specific energy consumption, yet the overall specific energy consumption in combined methods was lower than the traditional method. This may be due to the traditional method keeping the electric heater on for a longer duration than other methods, thereby increasing energy consumption. Furthermore, the significant heat loss around the electric heater when it was operational led to decreased energy efficiency, which ultimately increased specific energy consumption. The results still showed that solar energy (renewable energy) accounted for 54.91%, 52.62%, and 48.85% of the total energy consumption in the PRW-65, PRW-75, and PRW-85 combined methods, respectively; reducing the consumption of non-renewable energy by the same amount. Figure 5 illustrates the share of solar energy in each of the examined methods. In the SRW method, where all the energy for heating water was supplied by solar collectors, approximately 70.31% of the total energy consumption was attributed to solar energy. According to the results, in both RW and PRW methods, with an increase in temperature, although the drying time of the product decreased, the specific energy consumption showed an increasing trend. This could be attributed to the high specific heat capacity of water, which requires

more energy to raise its temperature to higher levels. This is contrary to what happened in past studies on convective drying, where reports showed that with an increase in the temperature of the hot air entering the dryer, the specific energy consumption mostly decreased (Samadi & Loghmanieh, 2013). Figure 4b illustrates the specific moisture extraction rate (SMER). The SMER ranged between 0.05-0.097 (kg kWh^{-1}) in various methods. The highest SMER value was obtained in the SRW method, while the lowest SMER was in the RW-85 method. The SMER decreased in both drying methods with an increase in temperature, mainly due to increased energy consumption and decreased efficiency at higher temperatures. In a similar study, the SMER for convective drying of kiwi was found to be in the range of 0.11-0.15 kg kWh^{-1} (Mohammadi *et al.*, 2019). Figures 4c and 4d show the energy efficiency and dryer efficiency in various drying methods, respectively. The lowest and highest energy efficiencies were 3.36% and 6.51%, obtained in the RW-85 and SRW methods, respectively. The traditional RW-65 and RW-85 methods had the highest and lowest energy efficiencies, respectively. In the combined method, PRW-65 had higher energy efficiency compared to other methods. The main factors contributing to the variations in results were the differences in drying time and the duration the electric heater was on. For example, in the RW-85 method, the electric heater operated for a longer duration compared to other methods. At this temperature level, the significant temperature difference between the inside and outside environments results in high heat losses. As a result, the electric heater must remain continuously on to maintain the desired temperature. According to the results, the lowest (6.76%) and highest (10.51%) drying efficiencies were obtained in the RW-85 and SRW methods, respectively. In the SRW method, due to reduced heat losses resulting from the electric heater being turned off, energy efficiency and drying efficiency increased, while in the RW-85 method, with the heater being on for a longer period and increased heat losses, both energy efficiency and drying efficiency decreased. Similarly, in another study, the energy efficiency and drying efficiency for convective drying of apples were found to be in the ranges of 2.87-9.11% and 3.49-12.29%, respectively (Beigi, 2016). Overall, these results indicate that in the traditional method, the energy efficiency is still low, and by utilizing solar energy, a significant portion of the non-renewable energy consumption is reduced.

Environmental Impact Assessment

In this study, the production of pollutants per kilogram of water removed from the product was calculated to assess the environmental impacts. The calculations were based on the energy consumption from renewable and non-renewable sources in the drying process, as well as the coefficients related to pollutant production in power plants in Iran per unit of energy produced. According to the results, the use of clean solar energy led to a significant reduction in pollutant emissions. Figure 6a illustrates the CO_2 emissions in various drying methods. The analysis showed that the highest CO_2 emissions were associated with the RW-85 method at 122.88 (kg kg $water^{-1}$), while the lowest emissions were related to the SRW method at 18.84 (kg kg $water^{-1}$). On average, using solar energy in PRW and SRW methods reduced CO_2 emissions by 54.64% and 80.94%, respectively, compared to the traditional method (RW). Similarly, to energy consumption in drying, the production of pollutants increased with the drying temperature in all methods. Figure 6b presents the SO_2 emissions for different drying methods. The investigation revealed that the highest SO_2 emissions were observed in the RW-85 method at 0.509 (kg kg $water^{-1}$), while the lowest emissions were in the SRW method at 0.078 (kg kg $water^{-1}$). The range of SO_2 emissions was between 0.285-0.509 (kg kg $water^{-1}$) in the traditional method and 0.164-0.215 (kg kg $water^{-1}$) in the solar combined (PRW) method. Similar to CO_2 emissions, the production of SO_2 increased with the drying temperature, and it was lower in the solar

combined (PRW) method compared to the traditional (RW) method. Figure 6c shows the CH_4 emissions in various drying methods. CH_4 is another significant greenhouse gas produced in power plants, which, despite its lower production compared to other gases, has significant environmental impacts. The highest CH_4 emissions were obtained in the RW-85 method at 29×10^{-4} (kg kg water^{-1}), while the lowest emissions were in the SRW method at 45×10^{-5} (kg kg water^{-1}). Similar to other pollutants, CH4 emissions decreased with the use of solar energy. The range of CH_4 emissions was between $16\text{-}29\times10^{-4}$ (kg kg water^{-1}) in the traditional method and $9\times10^{-4}\text{-}12\times10^{-4}$ (kg kg water^{-1}) in the solar combined (PRW) method. NOx emissions were also investigated in this study, as shown in Figure 6d. The highest NOx emissions were associated with the RW-85 method at 0.457 (kg kg water^{-1}), while the lowest emissions were in the SRW method at 0.07 (kg kg water^{-1}). The range of NOx emissions was between 0.256-0.457 (kg water^{-1}) in the traditional method and 0.147-0.193 (kg kg water^{-1}) in the solar combined (PRW) method. In a similar study, the total amounts of CO_2 and NOx emissions in microwave drying were reported to be 20.121 kg and 0.072 kg, respectively (Taghinezhad *et al.*, 2023).

Fig. 5. Share of non-renewable and renewable energy from energy consumption in different drying methods

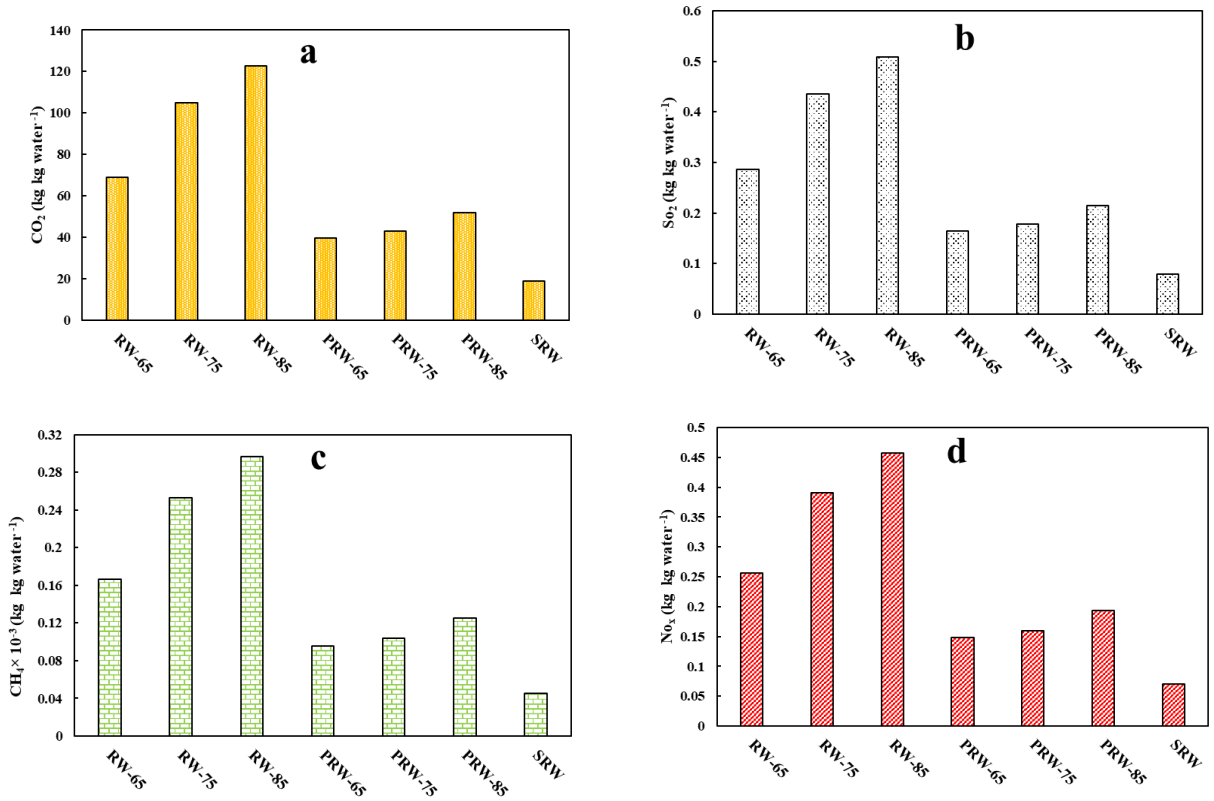

Fig. 6. The equivalent amount of pollutant emissions including: a) carbon dioxide, b) sulfur dioxide, c) methane, and (d) NOx in different drying methods

Conclusion

In this study, energy consumption and pollutant emissions for drying apple slices in a new hybrid solar dryer type RW-PTC were investigated. Drying was performed using three methods: the conventional Refractance Window drying method (RW), the combined drying method (PRW), and the fully solar method (SRW). The optical efficiency and thermal efficiency of the PTC collector during the experimental hours were determined to be 62.01% and 49.31%, respectively, which were slightly lower compared to a standard collector. Energy parameters indicated that solar energy in the PRW-65, PRW-75, PRW-85, and especially SRW drying methods significantly contributed to the total energy consumption and reduced reliance on non-renewable energy sources. On average, in the PRW and SRW methods of drying, CO_2 and other pollutants decreased significantly compared to the conventional RW. Overall, the RW-PTC system proved to be a suitable hybrid solar system for reducing fossil fuel consumption in dryers. With proper design and adjustment of concentration ratio (in the PTC collector), future research can optimize the inlet temperature to the dryer and increase the system efficiency.

Authors Contribution

M. Teymori-Omran:Data acquisition, Data pre and post processing, Statistical analysis, Software cervices

E. Askari Asli-Ardeh: Supervision, Conceptualization, Methodology

A. Motevali: Conceptualization, Technical advice, Review and editing services

E. Taghinezhad: Methodology, Text mining, Visualization

Nomenclature

A_{ac}	Aperture area of the collector (m^2)	$Q_{l,d}$	Thermal losses of dryer (kJ)
$C_{P,p}$	Specific heat of sample (kJ kg^{-1} $°C^{-1}$)	Q_P	Energy used for heating the product (kJ)
$C_{P,w}$	Specific heat of water (kJ kg^{-1} $°C^{-1}$)	SEC	Specific energy consumption (kWh kg^{-1})
DE	Drying efficiency (%)	$SMER$	Specific moisture extraction ratio (kWh kg^{-1})
D_{ro}	Receiver outer diameter (mm)	T_{out}	Outlet temperature (°C)
D_{ri}	Inner diameter (mm)	T_{in}	Inlet temperature (°C)
f	Focal length	W	Parabola width (m)
G_b	Direct beam radiation (W m^{-2})	α	Solar declination angle (°)
M	Moisture content (%)	β	Solar hour angle (°)
MR	Moisture ratio	γ	Intercept factor
M_0	Initial moisture content (%)	τ	Cover transmittance
M_e	Equilibrium moisture content (%)	ω	Absorber absorbance
m_f	Final weight of sample (g)	λ_l	Latent heat of vaporization of water (kJ kg^{-1})
m_i	Initial weight of sample (g)	ρ_T	Total reflectance
l	Parabola Length (m)	ϕ_r	Rim angle (°)
Q_S	Solar radiation on the PTC aperture (W m^{-2})	$X(\theta)$	Incident angle modifier (°)
Qu	Useful heat (W)	η_{opt}	Optical efficiency (%)
Q_{abs}	Absorbed thermal energy (W)	η_{th}	Thermal efficiency (%)
Q_{ev}	Energy used for moisture evaporation (kJ)		
Q_{loss}	Thermal losses of PTC (W)		

References

1. Awan, A. B., Khan, M. N., Zubair, M., & Bellos, E. (2020). Commercial parabolic trough CSP plants: Research trends and technological advancements. *Solar Energy*, *211*, 1422-1458. https://doi.org/10.1016/j.solener.2020.09.072
2. Baeghbali, V., Niakousari, M., & Farahnaky, A. (2016). Refractance Window drying of pomegranate juice: Quality retention and energy efficiency. LWT-Food science and technology, 66, 34-40. https://doi.org/10.1016/j.lwt.2015.10.017
3. Beigi, M. (2016). Energy efficiency and moisture diffusivity of apple slices during convective drying. Food Science and Technology (Campinas), 36(1), 145-150. https://doi.org/10.1590/1678-457X.0068
4. Bellos, E., & Tzivanidis, C. (2018). Enhancing the performance of evacuated and non-evacuated parabolic trough collectors using twisted tape inserts, perforated plate inserts and internally finned absorber. *Energies*, *11*(5), 1129. https://doi.org/10.3390/en11051129
5. Bellos, E., & Tzivanidis, C. (2020). Polynomial expressions for the thermal efficiency of the parabolic trough solar collector. *Applied Sciences*, *10*(19), 6901. https://doi.org/10.3390/app10196901
6. Camci, M. (2020). Thermodynamic analysis of a novel integration of a spray dryer and solar collectors: A case study of a milk powder drying system. *Drying Technology*, *38*(3), 350-360. https://doi.org/10.1080/07373937.2019.1570935
7. Caparino, O. A., Tang, J., Nindo, C. I., Sablani, S. S., Powers, J. R., & Fellman, J. K. (2012). Effect of drying methods on the physical properties and microstructures of mango (Philippine 'Carabao'var.) powder. *Journal of Food Engineering*, *111*(1), 135-148. https://doi.org/10.1016/j.jfoodeng.2012.01.010
8. Chafie, M., Aissa, M. F. B., & Guizani, A. (2018). Energetic end exergetic performance of a parabolic trough collector receiver: An experimental study. *Journal of Cleaner Production*, *171*, 285-296. https://doi.org/10.1016/j.jclepro.2017.10.012

9. Elmohlawy, A. E., Kazanjan, B. I., & Ochkov, V. F. (2018, November). Modeling and performance prediction of solar parabolic trough collector for hybrid thermal power generation plant under different weather conditions. In *AIP Conference Proceedings* (Vol. 2047, No. 1). AIP Publishing. https://doi.org/10.1063/1.5081635
10. Gaul, H., & Rabl, A. (1980). Incidence-angle modifier and average optical efficiency of parabolic trough collectors. Journal of solar energy engeenering. 16-21 https://doi.org/10.1115/1.3266115
11. Gharehdaghi, S., Moujaes, S. F., & Nejad, A. M. (2021). Thermal-fluid analysis of a parabolic trough solar collector of a direct supercritical carbon dioxide Brayton cycle: A numerical study. *Solar Energy*, *220*, 766-787. https://doi.org/10.1016/j.solener.2021.03.039
12. Kajavali, A., Sivaraman, B., & Kulasekharan, N. (2014). Investigation of heat transfer enhancement in a parabolic trough collector with a modified absorber. *International Energy Journal*, *14*(4).
13. Kalogirou, S. A. (2023). *Solar energy engineering: processes and systems*. Elsevier. 51-123. https://doi.org/10.1016/B978-0-12-397270-5.00002-9
14. Kumar, P., & Singh, D. (2020). Advanced technologies and performance investigations of solar dryers: A review. *Renewable Energy Focus*, *35*, 148-158. https://doi.org/10.1016/j.ref.2020.10.003
15. Mahanti, N. K., Chakraborty, S. K., Sudhakar, A., Verma, D. K., Shankar, S., Thakur, M., & Srivastav, P. P. (2021). Refractance Window-Drying vs. other drying methods and effect of different process parameters on quality of foods: A comprehensive review of trends and technological developments. *Future Foods*, *3*, 100024. https://doi.org/10.1016/j.fufo.2021.100024
16. Manikandan, G. K., Iniyan, S., & Goic, R. (2019). Enhancing the optical and thermal efficiency of a parabolic trough collector–A review. *Applied Energy*, *235*, 1524-1540. https://doi.org/10.1016/j.apenergy.2018.11.048
17. Mohammadi, I., Tabatabaekoloor, R., & Motevali, A. (2019). Effect of air recirculation and heat pump on mass transfer and energy parameters in drying of kiwifruit slices. *Energy*, *170*, 149-158. https://doi.org/10.1016/j.energy.2018.12.099
18. Motevali, A., Minaei, S., Banakar, A., Ghobadian, B., & Khoshtaghaza, M. H. (2014). Comparison of energy parameters in various dryers. *Energy Conversion and Management*, *87*, 711-725. https://doi.org/10.1016/j.enconman.2014.07.012
19. Nazari, S., Shahhoseini, O., Sohrabi-Kashani, A., Davari, S., Paydar, R., & Delavar-Moghadam, Z. (2010). Experimental determination and analysis of CO_2, SO_2 and NOx emission factors in Iran's thermal power plants. *Energy*, *35*(7), 2992-2998. https://doi.org/10.1016/j.energy.2010.03.035
20. Nindo, C. I., Feng, H., Shen, G. Q., Tang, J., & Kang, D. H. (2003). Energy utilization and microbial reduction in a new film drying system. *Journal of Food Processing and Preservation*, *27*(2), 117-136. https://doi.org/10.1111/j.1745-4549.2003.tb00506.x
21. Onwude, D. I., Hashim, N., Abdan, K., Janius, R., & Chen, G. (2019). The effectiveness of combined infrared and hot-air drying strategies for sweet potato. *Journal of Food Engineering*, *241*, 75-87. https://doi.org/10.1016/j.jfoodeng.2018.08.008
22. Padhi, S., & Dwivedi, M. (2022). Physico-chemical, structural, functional and powder flow properties of unripe green banana flour after the application of Refractance window drying. *Future Foods*, *5*, 100101. https://doi.org/10.1016/j.fufo.2021.100101
23. Raghavi, L. M., Moses, J. A., & Anandharamakrishnan, C. (2018). Refractance window drying of foods: A review. *Journal of Food Engineering*, *222*, 267-275. https://doi.org/10.1016/j.jfoodeng.2017.11.032
24. Rajoriya, D., Shewale, S. R., & Hebbar, H. U. (2019). Refractance window drying of apple

slices: Mass transfer phenomena and quality parameters. *Food and Bioprocess Technology*, *12*, 1646-1658. https://doi.org/10.1007/s11947-019-02334-7

25. Rajoriya, D., Shewale, S. R., Bhavya, M. L., & Hebbar, H. U. (2020). Far infrared assisted refractance window drying of apple slices: Comparative study on flavour, nutrient retention and drying characteristics. *Innovative Food Science & Emerging Technologies*, *66*, 102530. https://doi.org/10.1016/j.ifset.2020.102530
26. Samadi, S. H., & Loghmanieh, I. (2013). Evaluation of energy aspects of apple drying in the hot-air and infrared dryers. *Energy Research Journal*, *4*(1), 30-38. https://doi.org/10.3844/erjsp.2013.30.38
27. Seyfi, A., Asl, A. R., & Motevali, A. (2021). Comparison of the energy and pollution parameters in solar refractance window (photovoltaic-thermal), conventional refractance window, and hot air dryer. *Solar Energy*, *229*, 162-173. https://doi.org/10.1016/j.solener.2021.05.094
28. Shahraki, A., Khojastehpour, M., Golzarian, M. R., & Azarpazhooh, E. (2024). Simulation of Heat and Mass Transfer in a Refractance Window Dryer for Aloe vera gel. *Journal of Agricultural Machinery*, *14*(2), 197-214. https://doi.org/10.22067/jam.2023.80368.1141
29. Shirole, A., Wagh, M., & Kulkarni, V. (2021). Thermal Performance Comparison of Parabolic trough collector (PTC) using various Nanofluids. *International Journal of Renewable Energy Development*, *10*(4), 875. https://doi.org/10.14710/ijred.2021.33801
30. Sookramoon, K. (2016). Design of a Solar Tunnel Dryer Combined Heat with a Parabolic Trough for Paddy Drying. *Applied Mechanics and Materials*, *851*, 239-243. https://doi.org/10.4028/www.scientific.net/AMM.851.239
31. Taghinezhad, E., Kaveh, M., Szumny, A., Figiel, A., & Blasco, J. (2023). Qualitative, energy and environmental aspects of microwave drying of pre-treated apple slices. *Scientific Reports*, *13*(1), 16152. https://doi.org/10.1038/s41598-023-43358-6
32. Teymori-Omran, M., Askari Asli-Ardeh, E., Taghinezhad, E., Motevali, A., Szumny, A., & Nowacka, M. (2023). Enhancing Energy Efficiency and retention of bioactive compounds in apple drying: Comparative analysis of combined hot air–infrared drying strategies. *Applied Sciences*, *13*(13), 7612. https://doi.org/10.3390/app13137612
33. Teymori-omran, M., Motevali, A., Seyedi, S. R. M., & Montazeri, M. (2021). Numerical simulation and experimental validation of a photovoltaic/thermal system: Performance comparison inside and outside greenhouse. *Sustainable Energy Technologies and Assessments*, *46*, 101271. https://doi.org/10.1016/j.seta.2021.101271
34. Tiwari, S., Tiwari, G. N., & Al-Helal, I. M. (2016). Performance analysis of photovoltaic–thermal (PVT) mixed mode greenhouse solar dryer. *Solar Energy*, *133*, 421-428. https://doi.org/10.1016/j.solener.2016.04.033
35. Waghmare, R. (2021). Refractance window drying: A cohort review on quality characteristics. *Trends in Food Science & Technology*, *110*, 652-662. https://doi.org/10.1016/j.tifs.2021.02.030
36. Wang, Q., Yao, Y., Shen, Z., & Yang, H. (2023). A hybrid parabolic trough solar collector system integrated with photovoltaics. *Applied Energy*, *329*, 120336. https://doi.org/10.1016/j.apenergy.2022.120336

ارزیابی پارامترهای انرژی و گازهای آلاینده برای خشک کردن سیب در خشک‌کن خورشیدی رفرکتنس ویندو مجهز به یک کلکتور خورشیدی سهموی خطی

میلاد تیموری عمران[1]، عزت اله عسکری اصلی اردە[1*]، علی متولی[2]، ابراهیم تقی نژاد[3]

تاریخ دریافت: ۱۴۰۳/۰۸/۰۳
تاریخ پذیرش: ۱۴۰۳/۱۰/۱۰

چکیده

در این مطالعه، فرآیند خشک کردن سیب با استفاده از یک خشک‌کن خورشیدی ترکیبی جدید، از نوع خشک‌کن ترکیبی رفرکتنس ویندو مجهز به کلکتور سهموی خطی مورد بررسی قرار گرفت. سینتیک خشک کردن، بازدهی انرژی و نقش خشک‌کن در کاهش مصرف انرژی و انتشار گازهای آلاینده ارزیابی شد. آزمایش‌های خشک کردن با سه منبع انرژی شامل انرژی تجدیدناپذیر مرسوم (RW)، خشک کردن با کمک خورشیدی (PRW) و خشک کردن کامل خورشیدی (SRW) انجام شد. میانگین بازده اپتیکی نوری و بازده حرارتی کلکتور PTC در طول ساعات آزمایش به‌ترتیب ۶۲/۰۱٪ و ۴۹/۳۱٪ به‌دست آمد. کمترین مصرف انرژی ویژه در روش SRW به میزان ($kWh\ kg^{-1}$) ۱۰/۲۴به‌دست آمد. علاوه بر این، نتایج نشان داد که انرژی خورشیدی برای روش‌های خشک کردن ترکیبی PRW-65، PRW-75، PRW-85 و روش تماما خورشیدی SRW به‌ترتیب ۵۴/۹۱ ، ۵۲/۶۲ ، ۴۸/ ۸۵ و ۷۰/۳۰ ٪ از مصرف انرژی کل را به خود اختصاص داده و به همین مقدار از مصرف انرژی های تجدیدناپذیر کاهش دادند. با استفاده از کلکتور خورشیدی در روش‌های خشک کردن PRW و SRW، انتشار CO_2 به‌ترتیب ۵۴/۶۴ و ۸۰/۹۴ ٪ در مقایسه با روش RW معمولی کاهش یافت. به‌طور کلی، به‌کارگیری انرژی خورشیدی در روش‌های PRW و SRW باعث بهبود پارامترهای انرژی و کاهش انتشار آلاینده‌ها در طول فرآیند خشک‌کردن شد.

واژه‌های کلیدی: خشک کردن سیب، خشک‌کن خورشیدی، رفرکتنس ویندو، کلکتور سهموی خطی

۱- گروه مهندسی بیوسیستم، دانشگاه محقق اردبیلی، اردبیل، ایران
۲- گروه مهندسی بیوسیستم، دانشگاه علوم کشاورزی و منابع طبیعی ساری، ساری، ایران
۳- گروه مهندسی بیوسیستم، دانشکده کشاورزی، دانشگاه تربیت مدرس، تهران، ایران
(*- نویسنده مسئول: Email: ezzataskari@uma.ac.ir)

https://doi.org/10.22067/jam.2024.90300.1298